Transient Absorption Spectra and Dynamics of InSe Nanoparticles

Shuming Yang and David F. Kelley*

Division of Natural Sciences, University of California, Merced, Merced, California 95344

Received: March 26, 2006; In Final Form: May 17, 2006

Time-resolved fluorescence and transient absorption results have been obtained for small (∼3 nm) and large (∼5−8 nm) InSe nanoparticles in room-temperature solutions. The large particles are nonfluorescent, indicating that the conduction band is at M and the optical transition is forbidden. For some fraction of the small particles, the bottom of the conduction band is at Γ and the optical transition is allowed. The small particle fluorescence measurements indicate that hole trapping occurs on the 200−300 ps time scale. The transient absorption spectra are featureless throughout the visible with a broad maximum at 600−650 nm. The transient absorption kinetics of both small and large particles show a 200−300 ps decay component that is assigned to hole trapping. These kinetics also show a 15 ps decay that has a larger amplitude in the case of the large particles and is assigned to an electron Γ to M relaxation. The amplitude of this decay indicates that the initial electron and hole intraband transitions result in roughly comparable intensities of the initial transient absorption.

Introduction

Layered semiconductors are of great interest largely because they have highly anisotropic optical and electronic properties and have basal planes that are relatively inert. Because of these properties, layered semiconductors are often used as photochemical electrodes. Indium selenide (InSe) is a two-dimensional layered material having a D_{6h}^4 crystal structure.[1] This structure consists of covalently bonded Se−In−In−Se tetra-layer sheets, with the sheets held to each other by (primarily) van der Waals forces. The band gap of InSe is about $E_g = 1.24$ eV at room temperature,[2,3] which makes it an attractive material for solar energy conversion. Because of the absence of dangling bonds on the (001) surface, it has the potential to be used for heterojunction device applications with a low density of interface states.[4,5]

InSe is similar to GaSe; the two materials have the same crystal structure with similar lattice constants and similar electronic structures.[6,7] The electronic band structures of both materials have recently been calculated in the tight-binding approximation.[8] The electronic structure of InSe is qualitatively and in many places quantitatively similar to that of GaSe. Despite the similarities, there are some important differences in the electronic structures of these materials. The most significant differences are in the conduction band. Unlike GaSe, bulk InSe is a direct band gap material at Γ, with the M point in conduction band at slightly higher energy.[2,3,9,10] Furthermore, InSe has a smaller band gap and significantly stronger interlayer interactions, particularly for the conduction band electrons. The differences in the lowest conduction band momentum state and the extent of conduction band interlayer interactions turn out to be important in the transient absorption (TA) intraband spectroscopy discussed below.

In a previous paper, we reported the synthesis, characterization, and some aspects of the spectroscopy of 2.9, 4.7, and large InSe nanoparticles.[11] We showed that these nanoparticles have an unusual morphology: they consist of single tetra-layer Se−In−In−Se sheets. Because they are all single tetra-layer disks, the extent of *z*-axis (perpendicular to the basal planes) quantum confinement is the same. We found that the large particle absorption onset is about 7400 cm^{-1} to the blue of the bulk InSe band gap, indicative of *z*-axis quantum confinement. This value compares well with calculated 8685 cm^{-1} *z*-axis quantum confinement and corroborates the conclusion from electron diffraction, that particles are single tetra-layer disks. The previous study also found that fluorescence quantum yields increase with decreasing particle size. The smallest particles have quantum yields of typically 15−25%, and larger particles are essentially nonfluorescent. This is not due to faster trapping in the larger particles; the long-lived components of the fluorescence decays do not vary with particle size in any systematic way. This result suggests that the smallest particles have a direct band edge and the larger ones have an indirect band edge. This is not a surprising result. The top of the valence band in bulk InSe is at Γ, and the Γ and M points of the conduction band are close in energy. Small changes in the bonding and/or quantum confinement effects can alter the relative energetics of the conduction band Γ and M points. This conclusion is consistent with other aspects of the calculated band structure, as discussed below.

In previous papers, we have reported the transient absorption spectroscopy of GaSe nanoparticles.[12,13] These studies found that two types of transitions contribute to the transient absorption spectra. The largest GaSe particles are dominated by a *z*-polarized hole intraband transition. The smaller particles show the same *z*-polarized hole transition as well as an *x*,*y*-polarized electron absorption that is assigned to a conduction band to edge-state transition. The fluorescence and TA results also indicate that, in the case of the smallest GaSe particles, the bottom of the conduction band is at M rather than Γ; that is, the smallest particles have an indirect band gap. We found that, in this case, Γ to M electron relaxation dramatically affects the observed TA spectrum and its anisotropy.

In this paper, we report the time-resolved fluorescence and transient absorption spectroscopy of InSe nanoparticles. Specifically, we report results on several samples of small particles, having diameters of 2.8−3.6 nm, and several samples of

* Corresponding author. E-mail: dfkelley@ucmerced.edu.

10.1021/jp061870r CCC: $33.50
Published on Web 06/20/2006

approximately 5−8 nm particles. Some of these particles are the same ones used in the previously reported studies.[11] These results are analyzed in terms of the band structure of bulk InSe and a simple model for the intraband transitions of quantum-confined electrons and holes.

Experimental Section

Several of the samples used in the present study are the same as those used in our initial study of the static spectroscopy of InSe nanoparticles. In addition, several other samples were used that were synthesized using the same methods.[11] The results on small (2.8−3.6 nm) and larger (approximately 5−8 nm) particles are reported here. In most cases, the larger particles are size selectively precipitated with methanol, and subsequently redissolved in TBP or an octane/TOPO mixture (TBP = tributyl phosphine, TOPO = trioctyl phosphine oxide). The smaller particles are simply diluted in either TBP or an octane/TOPO mixture. The experimental apparatuses used to obtain the time-resolved fluorescence and transient absorption results are the same instruments as used in previous GaSe nanoparticle studies.[13,14] The only difference is that, in some of the results presented here, the larger InSe particles were excited at 505 nm, rather than 388 nm. In these cases, the pump pulse was generated with a Clark OPA.

In the case of the large particles, we found that the TA kinetics are power dependent at higher powers. Specifically, at the highest powers there is a fast decaying (1−2 ps) component. This is likely due to the formation of biexcitons. The results presented here were obtained at sufficiently low power to avoid this complication.

Results and Discussion

The basic idea of this study is to use the fluorescence decay results and the transient absorption (TA) decay kinetics to assign the electron and hole contributions in the InSe nanoparticle transient absorption spectra. If the observed fluorescence decay components can be assigned to respective electron and hole relaxation processes, then the contributions to the TA spectrum that decay with the same time constants can also be assigned. Below, we discuss the dynamical and spectroscopic manifestations of electron and hole relaxations processes. This is followed by an analysis and discussion of the experimental results on small and large particles. From the comparison of the small and large particle results, further assignments of the TA spectra can be made.

Fluorescence Polarization and the Band Structure of InSe. There are several different electron and hole relaxation processes that can affect both the fluorescence properties and the TA spectra of InSe nanoparticles. We will consider trapping and momentum relaxation in detail. Through these considerations, assignments of the relaxation processes observed in the fluorescence decays can be made. These assignments, along with the known band structure of InSe, are valuable in the subsequent assignment of the TA spectra and kinetics. To make these assignments, it is necessary to consider the structure of the InSe valence and conduction bands. Bulk InSe is a direct band gap semiconductor with the lowest energy transition at Γ. The bottom of the conduction band is split into Γ_3^+ and Γ_2^- levels by interlayer interactions.[6,8,10] (Although the single tetra-layer nanoparticles have D_{3h}^1 symmetry, for clarity and consistency, we will refer to the electronic states of both the bulk InSe and the nanoparticles in terms of the D_{6h}^4 symmetry of bulk β-InSe throughout this discussion.) This splitting is calculated to be about 7160 cm^{-1} and is, of course, not present in the case of these single tetra-layer particles.[8] The next conduction band levels (Γ_1^+ and Γ_4^-) are at considerably higher energy (calculated to be about 1.3 eV higher), are not optically accessible from the top of the valence band (Γ_4^-), and will not be considered further. The conclusion is that the Γ_3^+ and Γ_2^- conduction band levels are the only electron levels that need to be considered in the low-energy static spectroscopy of InSe. The valence band is more complicated. In the case of bulk InSe, the top of the valence band is at Γ and other momentum states are at much lower energy. The level at Γ is split into Γ_4^- and Γ_1^+ levels by interlayer interactions. This splitting is calculated to be about 9500 cm^{-1}. The optical transition from the top of the valence (Γ_4^-) to the bottom of the conduction band (Γ_3^+) is allowed and *z*-polarized.[15] At slightly lower energy (roughly 6200 cm^{-1}) are the $\Gamma_5^\pm$ and $\Gamma_6^\pm$ levels. The optical transition from the Γ_6^- to the bottom of the conduction band is allowed and *x*,*y*-polarized.[15] Thus, InSe shows two low energy absorptions: the lowest energy transition is *z*-polarized, and at slightly higher energy is an *x*,*y*-polarized transition. The qualitative structure of these bands is depicted in Figure 1. With these optical transitions in mind, it is of interest to consider fluorescence properties involving band edge versus trapped electrons and holes.

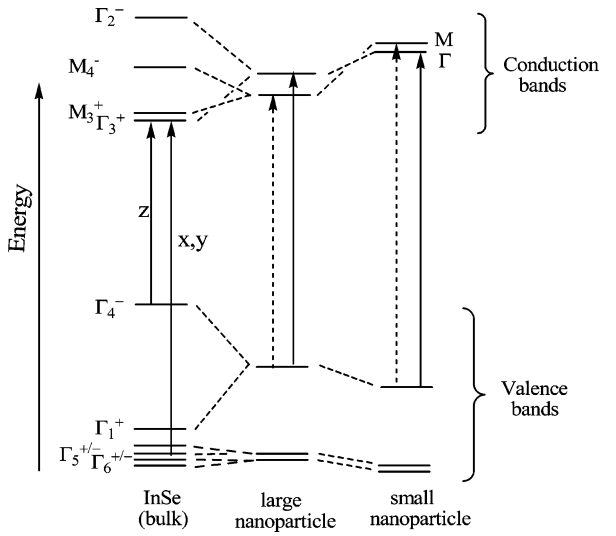

Figure 1. Energy level diagram of the valence and conduction bands of bulk InSe, large nanoparticles (only *z*-axis quantum confinement), and small nanoparticles (both *z*- and *x*,*y*-quantum confinement). Allowed transitions and their polarizations are shown for bulk InSe. Also shown are the allowed (solid arrows) and forbidden (dashed arrows) transitions from the top of the nanoparticle valence bands. The band gap is not to scale.

Trapping of the electron or hole will have the same qualitative effect on the fluorescence intensity; it will localize the electron or hole and thereby reduce the overlap with the other carrier. This results in a lower oscillator strength and therefore in diminished fluorescence intensity. Trapping of either the electron or the hole will therefore result in a fluorescence decay. The above band structure considerations also indicate that trapping of electrons or holes will have different effects on the fluorescence anisotropy. Band edge excitation and fluorescence involve the *z*-polarized $\Gamma_4^- - \Gamma_3^+$ transition and therefore will have an anisotropy close to 0.40.[16,17] (Spin−orbit coupling mixes in a small amount of the *x*,*y*-polarized $\Gamma_6^- - \Gamma_3^+$ transition, slightly lowering the observed anisotropy.[10]) In the case of a trapped electron, the only conduction band state in energetic proximity of the trap state from which oscillator strength can be derived is the conduction band edge, Γ_3^+. Thus, fluorescence involving electrons in shallow traps may be relatively weak,

but has the same polarization as if the electron were in the conduction band. The situation with fluorescence involving trapped holes is different. In this case, trapped hole transitions can derive oscillator strength from mixing with both the Γ_4^- and the Γ_6^- levels. Thus, fluorescence involving trapped holes will be weaker than band edge fluorescence, and because the two transitions from which transitions involving the trap state derives oscillator strength are of orthogonal polarizations, the fluorescence will be at least partially depolarized. Subsequent trap-to-trap hole relaxation can further depolarize the fluorescence. These considerations provide a way of experimentally separating electron and hole trapping dynamics; hole trapping depolarizes the fluorescence and electron trapping does not, and this is the critical observation in the assignment of these processes. We note that a relaxation process that depolarizes and decreases the fluorescence oscillator strength results in simple total (unpolarized) fluorescence decay kinetics (the unpolarized fluorescence decays at the relaxation time constant) but more complicated anisotropy kinetics. Thus, once the assignment to a hole trapping has been determined, the unpolarized fluorescence decay is the most straightforward measure of the hole trapping time. Similar arguments have been applied to the electron and hole trapping dynamics in GaSe nanoparticles.[14,18]

Relaxation Dynamics and the Band Structure of InSe. The relaxation processes that occur following photoexcitation depend critically on the relative energies of the conduction band Γ and M points. These states are close in energy in bulk InSe, with Γ being about 200 cm^{-1} lower.[3,9] Photoexcitation in all cases primarily puts the electron in the conduction band at Γ; the Γ−M optical transition is forbidden. If the M state is lower in the case of the nanoparticles, then, in addition to trapping, the conduction band electron at Γ can also undergo relaxation to M. Band structure considerations suggest that this will be the case for large single-tetra-layer nanoparticles. The interlayer splitting is much larger at Γ than M (7160 versus 2950 cm^{-1}, respectively[8]). However, Γ is only about 200 cm^{-1} lower than M in bulk InSe. This means that removal of the interlayer splitting is expected to raise the energy of the Γ point above that of the M point, as depicted in Figure 1. Consistent with this expectation, we find that the largest particles exhibit little or no fluorescence. The case of the small particles is more complicated because *x*,*y*-quantum confinement must also be considered.[11] The smallest particles exhibit strong fluorescence, indicating that, in at least some fraction of these particles, the bottom of the conduction band must be at Γ. Otherwise stated, the *x*,*y*-component of the electron effective mass is greater at Γ than M. We note that the fluorescence quantum yield of the small particles varies from one synthesis to another, further suggesting that these levels are close to each other. Small variations in the size distribution and/or surface chemistry can vary the fraction of particles for which the bottom of the conduction band is at Γ.

The TA assignments discussed below are based on the assertion that the electron intraband absorption in the 450−750 nm region is significant when the electron is at Γ and small when the electron is at M. This assertion follows from the magnitudes of the Γ and M interlayer splittings, derived from band structure calculations.[8] To explain the connection between the extents of interlayer interactions and the transient absorption spectrum, we must digress into the nature of the *z*-polarized electron and hole intraband transitions. In the simplest model, the electron or hole energy levels may be taken to be those of a particle-in-a-box; the length of the box is the thickness of the single tetra-layer particle. The zero-point energies may be estimated from the band structure calculations in the following way. The unit cell of bulk β-InSe consists of two tetra-layers. Bulk InSe states may have negative or positive symmetry with respect to reflection through the plane separating adjacent tetra-layers. The wave functions therefore have either constructive or destructive interference (i.e., a node) at the basal plane. In the case of the single tetra-layer nanoparticles, the wave function is neither forced to have a node nor does it constructively interfere with the wave function of an adjacent particle; it is halfway between these two extremes. Thus, the energy difference between the states split by interlayer interactions may be thought of as twice electron and hole *z*-axis quantum confinement energies in single tetra-layer particles. Alternatively, the electron (hole) *z*-axis quantum confinement energy may be thought of as the difference between the energy of the conduction (valence) band at the Γ and A points (where the interlayer interactions are zero). This Γ−A energy difference is one-half of the interlayer splitting at Γ depicted in Figure 1. The *z*-axis quantum confinement energy is the sum of the electron and hole zero-point energies, the energies of the particle-in-a-box $n = 1$ states. In this simple model, a *z*-polarized intraband transition is simply the $n = 1$ to $n = 2$ particle-in-a-box transition. It is important to note that the intraband transition energy is simply related to the *z*-axis quantum confinement energy and therefore to the interlayer energetic splitting of the bulk material states. The lowest electron or hole intraband transitions are at 3 times the *z*-axis quantum confinement energy of that carrier and therefore $^3/_2$ the conduction or valence band splitting induced by interlayer interactions. As a result, if this splitting is small, then the lowest energy transition will be at a low energy and no visible transient absorption will be observed. In the case of GaSe, there is a large interlayer splitting of the hole states (Γ_4^- and Γ_1^+), about 9500 cm^{-1}. As a result, a strong hole intraband transition is observed in the red region of the visible, peaking at about 15 000 cm^{-1}. GaSe has only a small splitting of the conduction band states (Γ_3^+ and Γ_2^-), and no *z*-polarized electron intraband transition is observed.[12,13] InSe has an almost identical 9500 cm^{-1} splitting of the Γ_4^- and Γ_1^+ valence band states, and a similar hole intraband spectrum is expected. However, in the case of InSe, the Γ_3^+ and Γ_2^- electron states exhibit a large splitting, about 7160 cm^{-1}, and a significant electron contribution to the visible TA spectrum is expected when the electron is at the Γ point. In contrast, the splitting of these levels at M (the M_4^+ and M_3^- states) is calculated to be much smaller, about 2950 cm^{-1}. Thus, no visible intraband absorption is expected when the electron is at the M point. As mentioned above, the bottom of the conduction band is at M in the case of large InSe nanoparticles. Photoexcitation initially puts the electron primarily at Γ, corresponding to the momentum allowed transition. In the case of the largest particles, a decrease in the TA intensity is expected as the electron relaxes from the Γ to the M point. In the case of the smaller particles, a significant fraction of the particles have the bottom of the conduction band at Γ, and a smaller amplitude of the Γ to M transient is expected. This expectation along with the hole trapping rates (determined from fluorescence measurements) allow unambiguous separation of the electron and hole contributions to the TA spectrum.

Fluorescence and Transient Absorption Spectra and Kinetics: Small Particles. Fluorescence from small (2.8−3.6 nm) particles is moderately intense, with quantum yields of typically 10−25%. Typical absorption and fluorescence spectra are presented in Figure 2. In contrast, 5−8 nm particles exhibit

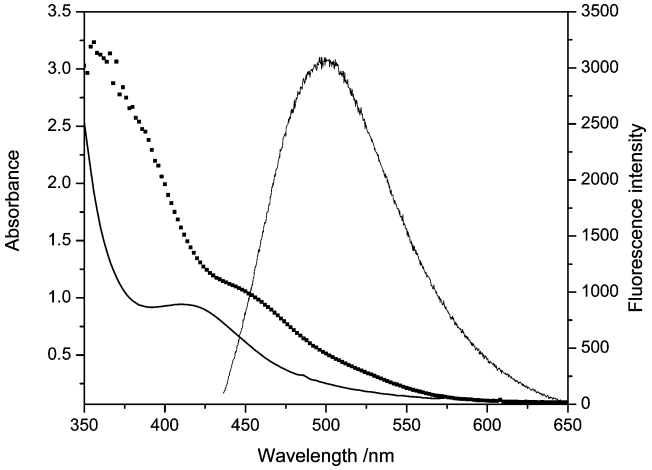

Figure 2. Static absorption spectra of small (solid curve) and large (dotted curve) InSe nanoparticles. The fluorescence spectrum of small nanoparticles excited at 430 nm is also shown.

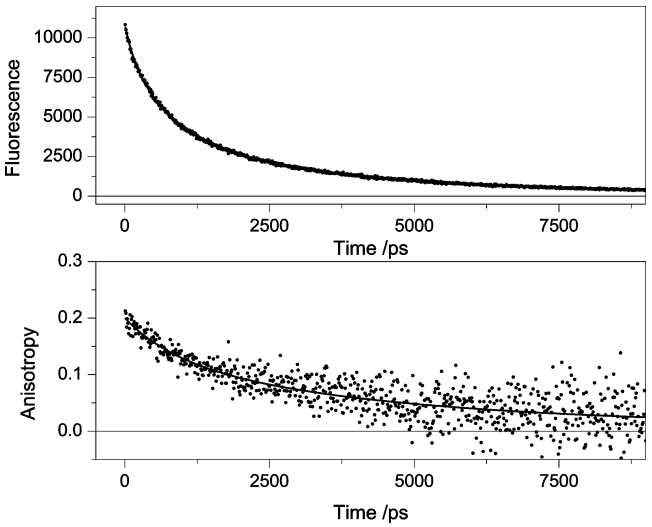

Figure 3. Fluorescence and fluorescence anisotropy kinetics of the small particles. Also shown is a curve fitted to the total emission decay having 200 ps, 900 ps, and 4.4 ns components, and a curve fitted to the anisotropy decay having the same time constants but different amplitudes.

little or no fluorescence and will not be considered further. Figure 3 shows that the small particle fluorescence decay following 380 nm excitation is characterized by approximately 200 ps (20%), 900 ps (54%), and 4.4 ns (26%) decay times. Consistent with emission decay kinetics, the fluorescence anisotropy decays may also be fit with the same time constants, and somewhat different relative amplitudes; see Figure 3. (We note that the initial anisotropy is considerably below the 0.40 limiting value because this excitation wavelength also excites some of the higher lying *x*,*y*-polarized transition, resulting in a loss of initial polarization. This excitation wavelength was chosen to be close to that used in the TA studies, and 430 nm excitation results in an initial fluorescence anisotropy of 0.32. This consideration also limits the quantitative use of polarization results in the TA spectra.) These decay kinetics indicate that hole trapping occurs on the 200 ps and longer time scales. The time resolution of this experiment is about 40 ps, and these results do not exclude the possibility of electron relaxation processes occurring on a faster time scale.

The TA spectrum of the small particles is broad with a peak at about 650 nm; see Figure 4. This is a difference spectrum and is due to a combination of intraband transitions, ground-

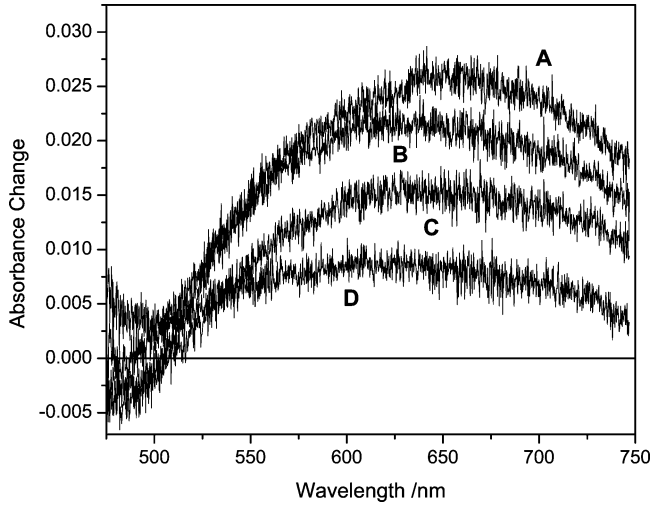

Figure 4. Transient absorption spectra of small nanoparticles at (A) 0 ps, (B) 15 ps, (C) 96 ps, and (D) 1000 ps following 388 nm excitation.

state bleach, and stimulated emission. All of these contributions are present at wavelengths less than about 575 nm, making this region of the spectrum difficult to interpret. The red (>600 nm) region of the spectrum is simpler, having only contributions from the intraband transitions. The absorption has a positive anisotropy, $r \approx 0.11$ for $\lambda > 600$ nm. Because band gap excitation is *z*-polarized, this indicates that the transition(s) giving rise to this transient absorption are dominantly *z*-polarized. The initial TA spectrum and anisotropy are reminiscent of what is observed for large GaSe nanoparticles,[12,13] the main difference being that the InSe TA spectrum has a somewhat larger absorption in the 500−600 nm region. The static absorption and fluorescence spectra of small InSe and large GaSe particles are not much different, indicating that this difference is largely due to a difference in the intraband absorptions. In the case of large GaSe particles, the transient absorption was assigned to (dominantly) a *z*-polarized $n = 1$ to $n = 2$ hole particle-in-a-box type transition. The similarities of the calculated valence band structures and TA spectra, particularly at $\lambda > 600$ nm, suggest that much of the InSe absorption may be assigned the same way. In the present case, the TA kinetics exhibit approximately 15 ps, 200−300 ps, and slow decays, as shown in Figure 5. Based on the fluorescence results, much of the slow decay components are assigned to hole trapping, consistent with the assignment that much of the absorption is due to a hole transition. In the 600−700 nm region, the 15 ps decay component is about 20% of the total decay. The magnitude of the fast component is somewhat variable from sample to sample. One sample of 2.8 nm particles exhibits slightly lower fluorescence quantum yields and also shows a somewhat larger 15 ps decay component, about 38%. In contrast, one strongly fluorescent sample (quantum yield greater than 30%) showed almost no fast component (less than a few percent) in the TA kinetics. These observations suggest that the fast component in the TA kinetics is associated with fluorescence quenching. The important point is that the small particle decays are dominated by the slow, hole trapping component and that, in these small particles, there is also a variable, but in all cases relatively small (<40%), fast decay component.

Transient Absorption Spectra and Kinetics: Large Particles. The absorption onsets of the larger particles are in the range of about 540−564 nm, indicating the different samples have average diameters ranging from 4.8 to about 8.0 nm. The time-resolved results presented here were obtained with a 4.8 nm sample (static absorption spectrum shown in Figure 2), but

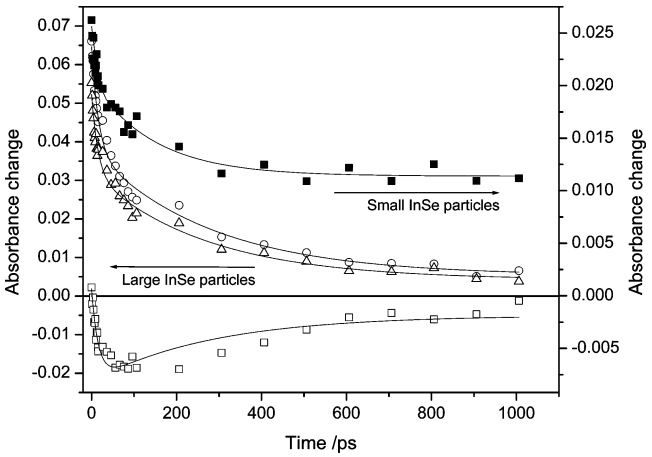

Figure 5. TA kinetics of small and large nanoparticles obtained at several different probe wavelengths following excitation at 388 nm. Specifically, small particles, 650 nm, ■; large particles 500 nm, □; 580 nm, ○; 700 nm, △. Also shown are fitted curves corresponding to the following: small particles, 650 nm, 16 ps (23%), 200 ps (31%), constant (46%); large particles 500 nm, 16 ps (100%), 280 ps (−71%), constant (−21%); 580 nm, 16 ps (42%), 280 ps (51%), constant (7%); 700 nm, 16 ps (38%), 280 ps (54%), constant (8%).

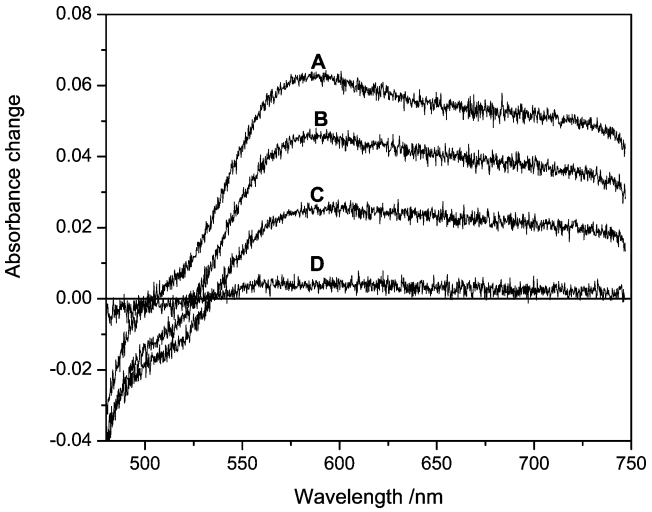

Figure 6. TA spectra of large nanoparticles at (A) 0 ps, (B) 15 ps, (C) 96 ps, and (D) 1000 ps following 388 nm excitation.

similar results are obtained on all of the larger particles. TA spectra of these particles excited at 388 nm are shown in Figure 6. This spectrum initially peaks at about 585 nm, significantly to the blue of the GaSe spectrum, and has considerably more intensity in the 500−580 nm region. The initial spectrum has a zero crossing point (where the magnitudes of the intraband absorptions and the ground-state bleach are equal) at about 505 nm. The blue absorbance decreases more rapidly than the red, and at longer times the zero crossing point shifts to 535 nm.

Figure 5 shows that the TA kinetics are detection wavelength dependent. The TA kinetics following 388 nm excitation show two transients: the 580 nm kinetics are fit with 16 ps (42%), 280 ps (52%), and constant (6%). Similar results are obtained at 700 nm. The 500 nm kinetics have the same time constants and about 1:−1 amplitude ratios. In this case, the initial transient gives an accurate assessment of the time constant of the fast, 16 ps component. The large amplitude fast component is characteristic of the large particles. We find that, in all cases, the large, nonfluorescent particles exhibit a significantly larger fast (12−16 ps) kinetic component than do the small particles. This is particularly true in the blue region of the spectrum, near 500 nm. The 500 nm kinetics indicate that these components have comparable amplitudes at that wavelength. It is of interest to note the 500 nm kinetics: the absorbance starts out near zero, goes quite negative, and slowly returns to zero. The above results make clear that there are spectrally distinct components to the observed transient absorptions and these components have kinetics that are particle size dependent. These results do not depend on the excitation wavelength. We find similar results following 505 nm excitation. Specifically, the decay at 650 nm is fit to 12 ps (55%) and 180 ps (45%) components. The differences are probably caused by the finite distribution of particle sizes and the size selectivity of 505 nm excitation.

Assignment of Electron and Hole Intraband Transitions. The above results suggest the initial transient absorption spectra have contributions from both electron and hole intraband transitions. The fluorescence decays establish that hole trapping occurs on the 200 ps and longer time scale. Thus, the part of the TA spectrum that decays on this time scale may be assigned to a hole intraband transition. This component is present in both small and large particles. The remainder of the observed absorption is assigned to an electron intraband transition, and the fast decaying (16 ps) transient is assigned to electron Γ to M relaxation and/or electron trapping. Based on the results presented here, there is no definitive way to separate the roles of Γ to M relaxation and electron trapping. However, the observation that the size-selectively precipitated large particles are always completely nonfluorescent indicates that the bottom of the conduction band is at M in these particles. Large and small particles are synthesized under similar conditions and therefore should have similar surface chemistries. Thus, there is no reason to expect that electron trapping should occur only in the largest particles. We therefore suggest that at least some and perhaps close to all of this transient is due to Γ to M relaxation. The above arguments indicate that the ordering of the Γ and M states reverses as the particles get smaller and that, in the small particles, the states are close in energy. We speculate that the reason that there is a small fast component in the small particles is that these particles are not completely monodisperse, and there is a finite concentration of larger particles. It may also be that the surface states affect the relative energies of the states at Γ and M and the surface chemistry varies slightly from particle to particle and from sample to sample. The conclusion is that this transient is due to some combination of electron trapping and Γ to M relaxation and that, in either case, the change of the transient absorption observed on the 15 ps time scale is due to the loss of the electron intraband absorption. With this assignment, the magnitude of the fast component in the large particles (on the order of 40−50%) indicates that electron and hole intraband transitions give rise to roughly comparable absorbances.

In the case of the large particles, the initial TA consists of components from both electron and hole intraband transitions; see Figure 6. The spectrum of the electron contribution can be inferred by comparison of the time-resolved spectra taken near $t = 0$ and at longer times when the electron contribution has decayed, but the hole contribution remains. This is done using the results in Figures 5 and 6 in the following way. The contribution from the electron intraband transition decays with a 16 ps time constant, so at 60 ps, only the hole contribution remains. The remaining spectrum decays with a 280 ps (51%) and long (7%) time constants. Knowing this decay rate, its contribution at $t = 0$ can be calculated and is just the 60 ps spectrum multiplied by a factor of 1.19 ($=0.51\ e^{60/280}/(0.51 + 0.07) + 0.07/(0.51 + 0.07)$. This spectrum and the $t = 0$

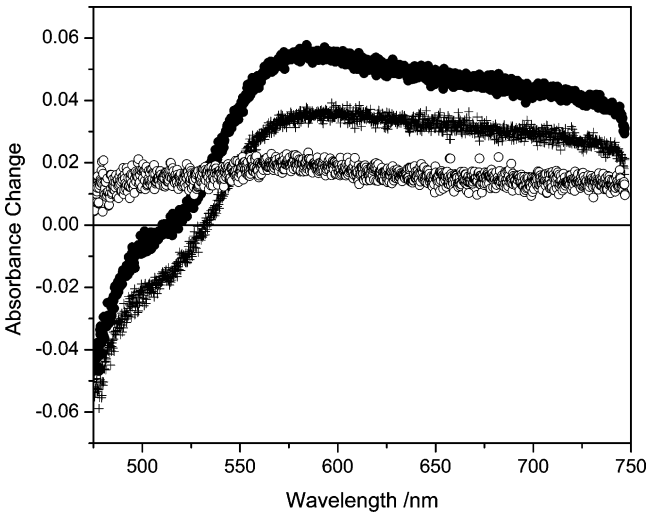

Figure 7. TA spectrum of the large particles at 0 ps (●), spectrum of the long-lived components extrapolated to $t = 0$ (+), and the difference spectrum corresponding to the fast component (○).

spectrum are shown in Figure 7. The rapidly decaying component of the spectrum is simply the difference between these spectra and is also shown in Figure 7. This spectrum is assigned to the electron intraband transition and is close to being flat over the entire spectral range, with an indistinct peak at about 575 nm. Based on the particle-in-a-cylinder model for *z*-axis quantum confinement and intraband transitions described above, the *z*-polarized electron transient absorption is expected to peak in the near-infrared, at about 930 nm. However, the observed spectrum shows a slight peak at about 575 nm. Other samples of large InSe nanoparticles show similar results. It is not clear if this discrepancy is due to inadequacies in the simple model or inaccuracies in the band structure calculations. It is also possible that *x*,*y*-polarized electron transitions may contribute to this absorption. Ongoing studies will further address this issue.

Summary and Conclusions

Several conclusions may be drawn from the results presented here.

(1) The fluorescence and fluorescence anisotropy decays indicate that, in the small InSe nanoparticles, hole trapping occurs on the 280 ps and longer time scale.

(2) The same 200−300 ps and longer time scale decay assigned to hole trapping is observed in the transient absorption decays of both the small and the large particles.

(3) In addition to the 280 ps transient, a much faster (12−16 ps) transient is also observed in the transient absorption kinetics. This transient is assigned to electron momentum relaxation and/or electron trapping.

(4) From the relative amplitudes of the fast and slow transients, the relative intensities of the electron and hole intraband transitions may be determined. We find that these intensities are comparable, with the hole transition giving somewhat more absorbance.

Acknowledgment. This work was supported by a grant from the Department of Energy, DE-FG03-00ER15037. We would also like to thank Dr. Haohua Tu for one sample of small InSe particles.

References and Notes

(1) Wieting, T. J.; Schluter, M. *Electrons and Phonons in Layered Crystal Structures*; Reidel: Dordrecht, 1979; Vol. 3.

(2) Camassel, J.; Merle, P.; Mathieu, H.; Chevy, A. *Phys. Rev. B* **1978**, *17*, 4718.

(3) Piacentini, M.; Doni, E.; Girlanda, R.; Grasso, V.; Balzarotti, A. *Nuovo Cimento* **1979**, *54B*, 269.

(4) Martinez-Pastor, J.; Segura, A.; Julien, C.; Chevy, A. *Phys. Rev. B* **1992**, *46*, 4607.

(5) Lang, O.; Klein, A.; Pettenkofer, C.; Jaegermann, W.; Chevy, A. *J. Appl. Phys.* **1996**, *80*, 3817.

(6) Schluter, M. *Nuovo Cimento* **1973**, *13B*, 313.

(7) Grasso, V. *Electronic Structure and Electronic Transitions in Layered Materials*; Reidel: Dordrecht, 1986.

(8) Camara, M. O. D.; Mauger, A.; Devos, I. *Phys. Rev. B* **2002**, *65*, 125206.

(9) Manjón, F. J.; Errandonea, D.; Segura, A.; Muñoz, V.; Tobías, G.; Ordejón; Canadell, E. *Phys. Rev. B* **2001**, *63*, 125330.

(10) Doni, E.; Girlanda, R.; Grasso, V.; Balzarotti, A.; Piacentini, M. *Nuovo Cimento* **1979**, *51B*, 154.

(11) Yang, S.; Kelley, D. F. *J. Phys. Chem. B* **2005**, *109*, 12701.

(12) Tu, H.; Chikan, V.; Kelley, D. F. *J. Phys. Chem. B* **2003**, *107*, 10389.

(13) Tu, H.; Mogyorosi, K.; Kelley, D. F. *Phys. Rev. B* **2005**, *72*, 205306.

(14) Chikan, V.; Kelley, D. F. *J. Chem. Phys.* **2002**, *117*, 8944.

(15) Koster, G. F.; Dimmock, J. O.; Wheeler, R. G.; Statz, H. *Properties of the Thirty-Two Point Groups*; M.I.T.: Cambridge, MA, 1963.

(16) Tao, T. *Biopolymers* **1969**, *8*, 609.

(17) Albrecht, A. *J. Mol. Spectrosc.* **1961**, *6*, 84.

(18) Chikan, V.; Kelley, D. F. *Nano Lett.* **2002**, *2*, 1015.